

Pulsewidth Modulation Method of Matrix Converter for Reducing Output Current Ripple

Sungmin Kim, *Student Member, IEEE*, Young-Doo Yoon, *Student Member, IEEE*,
and Seung-Ki Sul, *Fellow, IEEE*

Abstract—A matrix converter interfaces with three-phase ac voltage source, which creates three different virtual dc-link voltages. In this paper, a new pulsewidth modulation (PWM) method for the matrix converter is proposed to generally use these three virtual dc-link voltages. By using the two higher line-to-line voltages as the virtual dc-link voltages, the proposed method can create the identical switching sequences to those created by the conventional space vector PWM (SVPWM) method. Moreover, the proposed method is able to select the appropriate virtual dc-link voltage, according to the PWM purpose and/or load condition. In this paper, the virtual dc-link voltages adjacent to the output voltage reference are introduced to reduce output-current switching ripples. The feasibility of the proposed PWM method was verified by a computer simulation and experimental results. The output voltage and current waveforms produced by using the proposed method can be equal or better than those created using the conventional SVPWM method. Moreover, a new switching sequence that reduces output-current switching ripple can be easily adopted within the proposed PWM method. The harmonic characteristics of output current created using the proposed method are markedly improved over those using the conventional PWM method.

Index Terms—Current harmonics, matrix converter, pulsewidth modulation (PWM).

I. INTRODUCTION

A MATRIX converter is a direct ac–ac power converter employing nine bidirectional switches. In addition to its basic capacity to provide variable sinusoidal voltages to a load, a matrix converter has several attractive features: no bulky dc-link capacitor, the production of sinusoidal input current, high efficiency, compact circuit design, and regeneration capability. Despite these advantages, matrix converter has not been popular in industry because of the complexity in control of many bidirectional switches.

Since the early 1980s, several pulsewidth modulation (PWM) methods to control matrix converter have been proposed. First, Alesina and Venturini proposed a matrix-converter-control method using a mathematical approach to generate the desired output waveform [1]. After that, the authors extended the volt-

age transfer ratio from 0.5 to 0.866, which is the physical limit of matrix converter.

Since then, a well-known space vector PWM (SVPWM) method for a matrix converter has been proposed [2], [3]. Despite its many advantages as a common method, the SVPWM method of matrix converter requires complex calculations and tables. On the other hand, a different concept of SVPWM method was introduced, which is known as “indirect method,” where the matrix converter is interpreted as a cascade connection of two converters, a PWM converter, and a PWM inverter [4], [5]. In this approach, the PWM converter is interfaced with an ac voltage source and provides three virtual dc-link voltages, while the associated PWM inverter synthesizes the desired output voltage using these virtual dc-link voltages. Therefore, the SVPWM concept that is well established for voltage-source inverter could be extended to the matrix converter [6]. However, the requirement of numerous calculations and tables also remains as drawbacks of indirect method. To simplify the modulation procedure, Yoon and Sul proposed a carrier-based modulation technique, which was mathematically proven to be equivalent to the SVPWM method [7].

In the meantime, some researches on the PWM method concentrated in reduction of the switching loss and the improvement of the output-current quality have been introduced [8]–[14]. In [8], loss of matrix converter was reduced by minimizing the amount of switching. Furthermore, Helle *et al.* introduced another method for switching-loss reduction, which used minimized switching voltage [9]. The main idea of that research was to use the minimum line-to-line voltage when the output voltage reference was less than half of the input voltage. Similar approaches were also presented on the sparse matrix converter [10], [11]. Like Helle’s paper, the smallest and the second largest input line-to-line voltage were used as virtual dc-link voltages in the case of the low output voltage reference. These approaches can result in the reduced harmonics of the output voltages and output currents, and the decreased switching losses. Because these methods were based on the conventional SVPWM method, however, they also required complex calculations and switching combination tables. Furthermore, they would only be applicable when the output voltage reference is small.

Another method to reduce the switching losses using the predictive technique was proposed in [12] and [13]. The idea was to predict switching losses for every switching state, and then, selected the optimum state based on the evaluation criterion.

As a way to improve the output current characteristics, research on the arrangement of the zero vector was introduced in [14]. The geometrical analysis of the output current ripple

Manuscript received July 7, 2009; revised October 27, 2009; accepted January 22, 2010. Date of current version September 17, 2010. Recommended for publication by Associate Editor P. C. Loh.

The authors are with the School of Electrical Engineering, Seoul National University, Seoul 151-742, Korea (e-mail: ksmin@eepl.snu.ac.kr; birdy003@eepl.snu.ac.kr; sulsk@plaza.snu.ac.kr).

Color versions of one or more of the figures in this paper are available online at <http://ieeexplore.ieee.org>.

Digital Object Identifier 10.1109/TPEL.2010.2042179

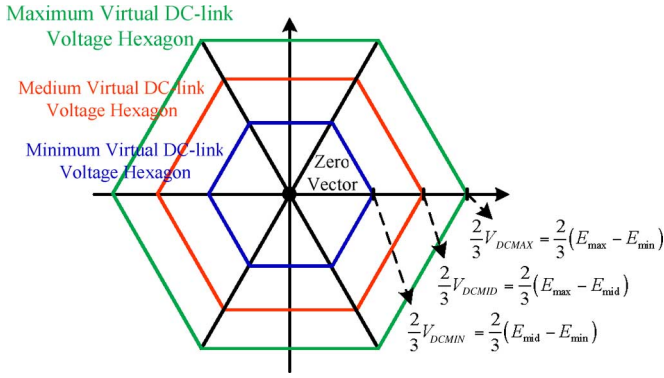


Fig. 1. Three Hexagons with virtual dc link in the voltage space plane.

showed a relationship between the current ripple and the zero-voltage vector. Moreover, this research indicated that an optimal arrangement of the zero-voltage vector can reduce the output current harmonics.

Among the foci of these previous researches on the matrix converter—the PWM method, the loss reduction, and the improvement in output current characteristics, this paper focuses on the PWM method as a technique to synthesize the output reference voltage and to make the input current sinusoidal. The purposes of this paper are two-folds, which are as follows.

- 1) To present a new generalized PWM method that uses three instantaneous virtual dc-link voltages.
- 2) To present a new switching sequence to reduce output current ripple as an application of the new generalized PWM method.

To verify the feasibility of the proposed PWM method, the identical switching sequences of the proposed PWM method with that of the conventional PWM was demonstrated without any tables and complex calculation. Then, to improve the output-current harmonic characteristics, a new switching sequence was generated based on the proposed PWM method, and then, experimentally verified.

II. PROPOSED PWM METHOD

A. Principle of the Proposed PWM Method

A matrix converter has three virtual dc-link voltages, which are generated by three line-to-line input voltages. As shown in Fig. 1, there are three instantaneous voltage hexagons in space vector plane, according to three-phase input line-to-line voltages. These three voltage hexagons are similar to those of a multilevel voltage-source inverter that has three dc-link voltages. Until now, the conventional PWM method has utilized effective voltage vectors only from the two larger virtual dc-link voltages and the zero-voltage vector using complex calculations and tables. To use the third virtual dc-link voltage vector, the conventional PWM method would require additional calculations and tables [9]. However, the PWM method proposed here introduces four general effective duty-ratio equations related to the three virtual dc-link voltages and the zero voltage. The four effective duty-ratio equations present the duty-ratio conditions necessary to synthesize the output voltage as the reference and

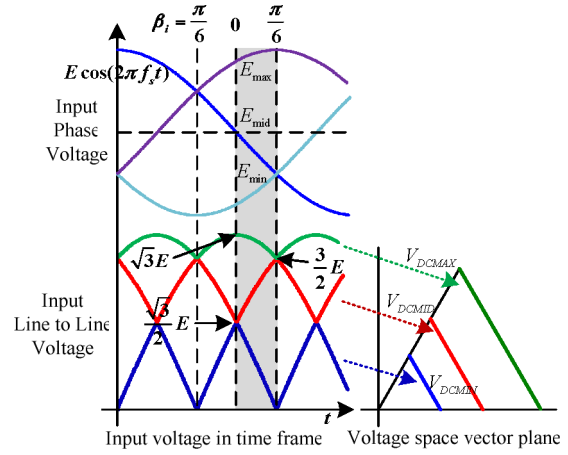
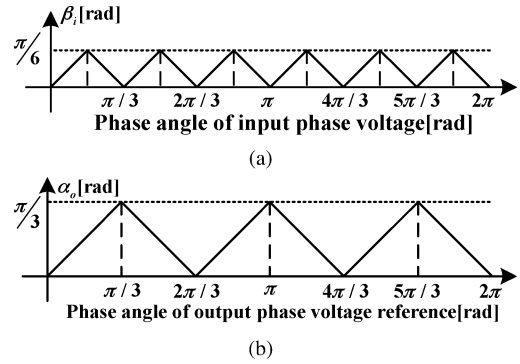


Fig. 2. Input line-to-line voltage, phase voltage, and virtual dc-link voltage.


 Fig. 3. Definition of phase angle of input voltage and output voltage reference. (a) Relation between β_i and phase angle of input phase voltage. (b) Relation between α_o and phase angle of output phase voltage reference.

to make the input currents be sinusoidal. Therefore, the proposed PWM method can select the appropriate virtual dc-link voltages, according to the purpose and/or load condition of the PWM.

B. Instantaneous Virtual DC-Link Voltages

In Fig. 2, the three input line-to-line voltages are shown along with the three input phase voltages. Because each input line-to-line voltage can be considered as a virtual dc-link voltage, the space-vector voltage plane of the matrix converter can be described, as shown in Fig. 2. In Fig. 2, E_{\max} , E_{mid} , and E_{\min} are defined as (1), and the instantaneous virtual dc-link voltages in the shaded area of Fig. 2 are calculated as (2). E means the peak value of the input phase voltage and f_s is the frequency of input voltage. The virtual dc-link voltages are repeated 12 times in one input-voltage period. Therefore, the phase angle of the input voltage can be converted to β_i in Fig. 3(a) for simple equations

$$E_{\max} = \text{MAX}[E_A, E_B, E_C] = E \sin\left(\beta_i + \frac{2}{3}\pi\right)$$

$$E_{\text{mid}} = \text{MID}[E_A, E_B, E_C] = E \sin\left(\beta_i + \frac{1}{3}\pi\right)$$

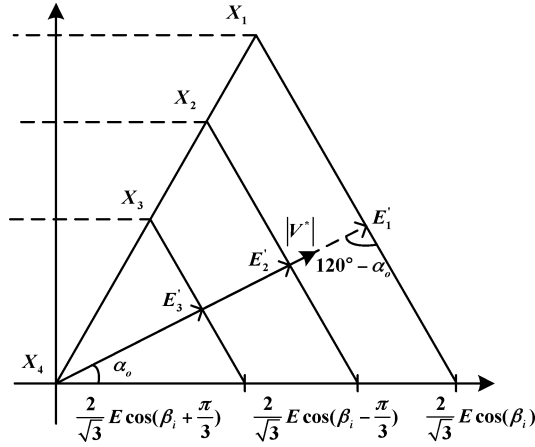


Fig. 4. Instantaneous space-vector voltage plane.

$$E_{\min} = \text{MIN} [E_A, E_B, E_C] = E \sin(\beta_i) \quad (1)$$

$$V_{\text{dcMAX}} = E_{\text{MAX}} - E_{\text{MIN}} = \sqrt{3}E \cos(\beta_i)$$

$$V_{\text{dcMID}} = E_{\text{MAX}} - E_{\text{MID}} = \sqrt{3}E \cos\left(\beta_i - \frac{\pi}{3}\right)$$

$$V_{\text{dcMIN}} = E_{\text{MID}} - E_{\text{MIN}} = \sqrt{3}E \cos\left(\beta_i + \frac{\pi}{3}\right). \quad (2)$$

C. Output Voltage Synthesis

The main purposes of a matrix converter are to synthesize the desired output voltage and to produce a sinusoidal input current. In Fig. 4, sextants of three hexagons in the space-vector voltage plane are shown. The magnitude of each hexagon is also displayed and the magnitude of three hexagons changes according to β_i , the phase angle of the input phase voltage. The output voltage reference can be described using polar coordinates as in (3), where $|V|$ is the magnitude of the output voltage reference vector and α_o , the phase angle of the output voltage reference is defined, as shown in Fig. 3(b)

$$V_{\text{reference}} = |V| \angle \alpha_o \quad (3)$$

$$E'_1 = \frac{E \cos(\beta_i)}{\sin((2/3)\pi - \alpha_o)}, \quad E'_2 = \frac{E \cos(\beta_i - (\pi/3))}{\sin((2/3)\pi - \alpha_o)},$$

$$E'_3 = \frac{E \cos(\beta_i + (\pi/3))}{\sin((2/3)\pi - \alpha_o)} \quad (4)$$

where E'_1 , E'_2 , and E'_3 represent the maximum voltage magnitudes from the corresponding virtual dc-link voltages without overmodulation. When the phase angle of the output voltage reference vector is α_o , the E'_1 , E'_2 , and E'_3 voltages may be described, as in (4). In Fig. 4, X_1 , X_2 , X_3 , and X_4 are the effective duty ratios in a switching period for the corresponding virtual dc-link voltages and the zero vector. Here, the X 's represent duty ratios in which the utilized virtual dc-link voltages are at maximum, medium, minimum, and zero magnitudes, respectively. The sum of the four X should be one.

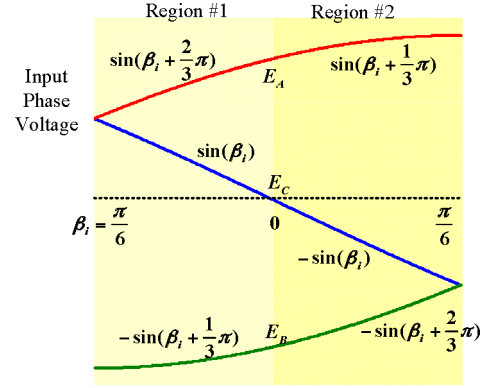


Fig. 5. Input voltage for phase angle 60° .

When the output voltage reference is given by (3), the magnitude $|V|$ can be expressed, as given in (5). However, by using (4), $|V|$ may be recalculated, as given in (6). The voltage transfer ratio q can be deduced, as given in (7)

$$|V| = E'_1 X_1 + E'_2 X_2 + E'_3 X_3 \quad (5)$$

$$|V| = \frac{E}{\sin((2\pi/3) - \alpha_o)} \times \left(\cos(\beta_i) X_1 + \cos\left(\beta_i - \frac{\pi}{3}\right) X_2 + \cos\left(\beta_i + \frac{\pi}{3}\right) X_3 \right) \quad (6)$$

$$q = \frac{|V|}{E}$$

$$= \frac{1}{\sin((2\pi/3) - \alpha_o)} \left(\cos(\beta_i) X_1 + \cos\left(\beta_i - \frac{\pi}{3}\right) X_2 + \cos\left(\beta_i + \frac{\pi}{3}\right) X_3 \right). \quad (7)$$

D. Sinusoidal Input Current Synthesis

To produce a sinusoidal input current and to have input power factor as one, the input current should be in phase with the input phase voltage. In the matrix converter, the input current is synthesized according to the segments of the output current via switching. In order to make the input current sinusoidal, the time duration of the connection of each input phase to the output current needs to be determined by the duty ratios X_1 , X_2 , X_3 , and X_4 . Region 1 of Fig. 5 indicates that the maximum input line-to-line voltage is $(E_A - E_B)$, the medium line-to-line voltage is $(E_C - E_B)$, and the minimum line-to-line voltage is $(E_A - E_C)$. During X_1 , which is the duty ratio when the maximum input line-to-line voltage is utilized, the input current flows from E_A and returns to E_B , as shown in Fig. 6(a). During X_2 , the input current flows from E_C and returns to E_B , as shown in Fig. 6(b), while during X_3 , input current flows from E_A and returns to E_C , as shown in Fig. 6(c). Thus, the resultant time duration of each input phase is determined by the duty ratios.

In order to achieve sinusoidal input currents with a power factor, the durations should be sinusoidal functions, which are related with input phase angle β_i . Therefore, the duty-ratio equations can be described as (8)–(10), where T is a constant that

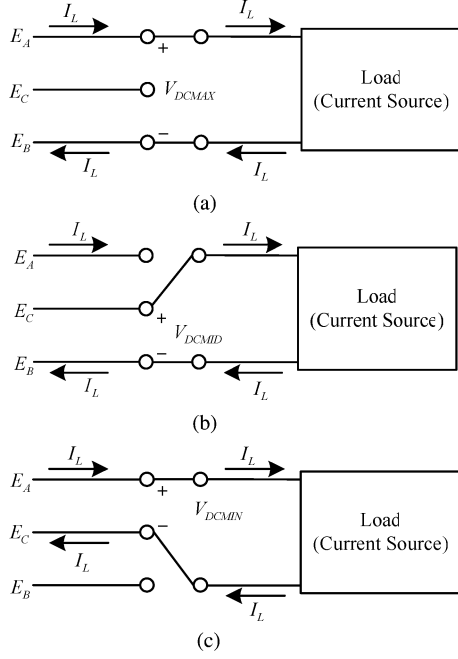


Fig. 6. Input current flow in matrix converter. (a) Input current flow during X_1 . (b) Input current flow during X_2 . (c) Input current flow during X_3 .

is proportional to the ratio between the magnitude of the input voltages and the output voltage reference at every switching period

$$\begin{aligned} \text{A phase: } I_L X_1 + I_L X_3 &= I_L \sin\left(\beta_i + \frac{2\pi}{3}\right) T \\ \Rightarrow X_1 + X_3 &= \sin\left(\beta_i + \frac{2\pi}{3}\right) T \end{aligned} \quad (8)$$

$$\begin{aligned} \text{B phase: } I_L X_1 + I_L X_2 &= I_L \sin\left(\beta_i + \frac{\pi}{3}\right) T \\ \Rightarrow X_1 + X_2 &= \sin\left(\beta_i + \frac{\pi}{3}\right) T \end{aligned} \quad (9)$$

$$\begin{aligned} \text{C phase: } I_L X_2 - I_L X_3 &= I_L \sin(\beta_i) T \\ \Rightarrow X_2 - X_3 &= \sin(\beta_i) T. \end{aligned} \quad (10)$$

Region 2 of Fig. 5 shows that the medium line-to-line voltage and the minimum line-to-line voltages are reversed. As a result, the duty ratios related to the each input phase should be changed; however, the duty-ratio equations are identical to (8)–(10). Thus, these equations can be rewritten as follows:

$$X_1 = -X_3 + \sin\left(\beta_i + \frac{2\pi}{3}\right) T \quad (11)$$

$$X_2 = X_3 + \sin(\beta_i) T. \quad (12)$$

E. Effective Duty-Ratio Equations

Equation (7) defines the conditions needed to synthesize the output voltage reference, while (8)–(10) present the relationships between effective duty ratios and input phase currents. By solving (7), (11), and (12) under the constraints of (13) and (14),

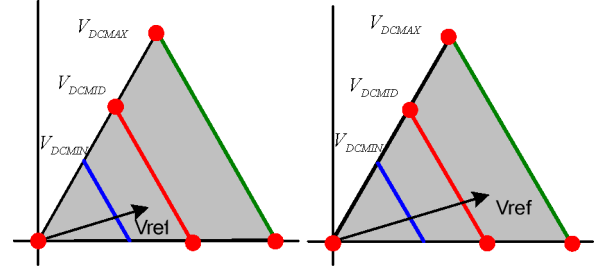


Fig. 7. Effective voltage vector of the conventional SVPWM at (a) small output voltage and (b) large output voltage.

the effective duty ratios can be described, as given in (15) and (16)

$$0 \leq X_1, X_2, X_3, X_4 \leq 1 \quad (13)$$

$$X_1 + X_2 + X_3 + X_4 = 1 \quad (14)$$

$$X_1 = -X_3 + \frac{2}{\sqrt{3}} q \sin\left(\frac{2\pi}{3} - \alpha_o\right) \sin\left(\beta_i + \frac{2\pi}{3}\right) \quad (15)$$

$$X_2 = X_3 + \frac{2}{\sqrt{3}} q \sin\left(\frac{2\pi}{3} - \alpha_o\right) \sin(\beta_i). \quad (16)$$

Effective duty-ratio equations are deduced from the output voltage synthesis and sinusoidal input current synthesis conditions. Therefore, if the effective duty ratios satisfy (13)–(16), then the input current would be sinusoidal and the output voltage would be synthesized as desired. The three effective duty-ratio equations (14)–(16) contain four undefined variables X_1 , X_2 , X_3 , and X_4 . In the proposed PWM method, one of these four variables can be used to create a degree of freedom that will result in a PWM performance improvement.

III. PWM SWITCHING SEQUENCE IN PROPOSED PWM METHOD

The proposed PWM method is a generalized method that uses the effective voltage vectors from all three virtual dc-link voltages and the zero-voltage vector. The method allows the proper switching sequence to be chosen, according to the PWM purpose. When the conventional SVPWM method is required, the proposed PWM method with $X_3 = 0$ can be utilized. The switching sequence developed by the proposed method is identical with that using the conventional SVPWM method. Moreover, in order to improve the output-current harmonic characteristics, a new switching sequence can be adopted. In the proposed method, when the magnitude of the output voltage reference is small, X_1 can be set to 0, and when the magnitude of output voltage reference is large, X_4 can be set to 0. This allows for seamless transitions among all switching sequences.

A. Switching Sequences Identical to Conventional PWM Method Sequences

Fig. 7 shows sextants of the virtual dc-link voltage hexagons under two output voltage reference magnitudes. Fig. 7(a) and (b) shows the virtual dc-link voltage vector with the conventional PWM method when output voltage is small or large,

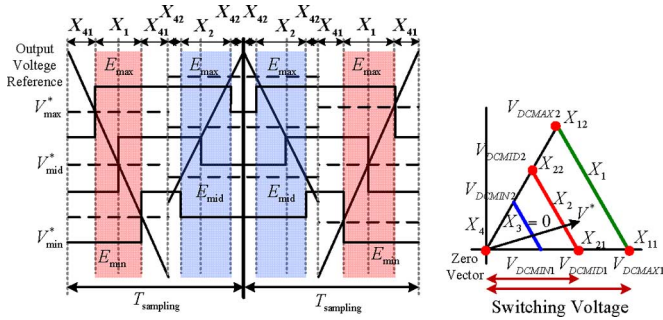


Fig. 8. Identical switching sequence with conventional method using proposed method. (a) Switching sequence. (b) Effective voltage vector.

respectively. In that method, the effective voltage vectors from the maximum and the medium virtual dc-link voltages, and the zero voltage are used, regardless of the magnitude of the output voltage reference vector.

To use three virtual dc-link voltages freely, the general effective duty-ratio equations that produce an output voltage as the output voltage reference and synthesize a sinusoidal input current can be applied. In such a case, when X_3 is set as zero, X_1, X_2 , and X_4 can be calculated from (13)–(16). Then, by applying the proper switching arrangement, as shown in Fig. 8, a switching sequence identical with that in the conventional SVPWM method [7] can be obtained.

The effective duty ratio of the maximum virtual dc-link voltage X_1 is a sum of two effective duty ratios X_{11} and X_{12} of two effective voltage vectors $V_{\text{dcMAX}1}$ and $V_{\text{dcMAX}2}$, respectively, as shown in Fig. 8(b). X_{11} and X_{12} can be calculated using (17) and (19) by adapting the carrier-based PWM method [7]. Similarly, X_2 is the sum of the X_{21} and X_{22} effective duty ratios, which can be calculated using (18) and (20). Here, $V_{\text{max}}^*, V_{\text{mid}}^*$, and V_{min}^* represent the maximum, medium, and minimum output voltage references, while $E_{\text{max}}, E_{\text{mid}}$, and E_{min} represent the maximum, medium, and minimum input phase voltages. In this switching sequence, there are six commutations during a switching period

$$X_1 = X_{11} + X_{12} \quad (17)$$

$$X_2 = X_{21} + X_{22} \quad (18)$$

$$X_{11} = X_1 \left(1 - \frac{V_{\text{mid}}^* - V_{\text{min}}^*}{V_{\text{max}}^* - V_{\text{min}}^*} \right) \quad (19)$$

$$X_{21} = X_2 \left(1 - \frac{V_{\text{mid}}^* - V_{\text{min}}^*}{V_{\text{max}}^* - V_{\text{min}}^*} \right). \quad (20)$$

In order to minimize the output current ripple, the zero-voltage vector should be properly arranged between the effective voltage vectors [12]. When the switching current ripple is simply calculated using (21), the output current ripples related with X_1 and X_2 can be expressed by (22) and (23), respectively. Because the zero-voltage vector should be distributed in proportion to the corresponding ripple current from the effective voltage vector, the zero-voltage vectors of the maximum and medium virtual dc-link voltages can be calculated, as in (25) and (26),

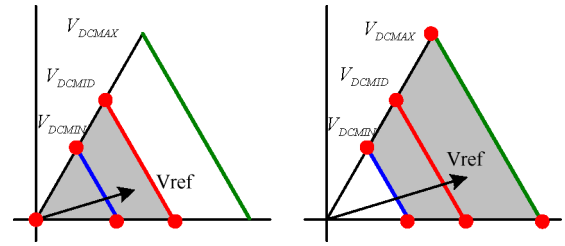


Fig. 9. Effective voltage vector of the proposed method for reducing output current ripple at (a) small output voltage and (b) large output voltage.

respectively,

$$L \frac{dI}{dt} = V_{\text{Switching}} \quad (21)$$

$$I_{\text{ripple1}} = \frac{1}{L} X_1 T_{\text{sampling}} V_{\text{dcMAX}} \quad (22)$$

$$I_{\text{ripple2}} = \frac{1}{L} X_2 T_{\text{sampling}} V_{\text{dcMID}} \quad (23)$$

$$I_{\text{ripple1}} : I_{\text{ripple2}} = V_{\text{dcMAX}} X_1 : V_{\text{dcMID}} X_2 \quad (24)$$

$$X_{41} = \frac{1}{2} T_{\text{sampling}} X_4 \frac{V_{\text{dcMAX}} X_1}{V_{\text{dcMAX}} X_1 + V_{\text{dcMID}} X_2} \quad (25)$$

$$X_{42} = \frac{1}{2} T_{\text{sampling}} X_4 \frac{V_{\text{dcMID}} X_2}{V_{\text{dcMAX}} X_1 + V_{\text{dcMID}} X_2}. \quad (26)$$

B. New Switching Sequences for Reduction of Output Current Ripple

In the proposed PWM method, a variety of PWM switching sequences can be implemented. One effective way to reduce the output current ripple is to minimize the voltage difference between the output voltage reference and the output voltage vector during a switching period. Therefore, new switching sequences that reduce output current ripple can be implemented using the effective voltage vectors adjacent to the output voltage reference.

Fig. 9 shows the dc-link voltages adjacent to the output voltage reference. When the magnitude of the output voltage reference vector is small, the effective voltage vectors from the medium and minimum virtual dc-link voltages and the zero-voltage are used, as shown in Fig. 9(a). In such a case, the effective voltage vectors from the maximum virtual dc-link voltage are not used. Similarly, when the magnitude is large, instead of using the zero-voltage vector, the effective voltage vectors from the three virtual dc-link voltages are used, as shown in Fig. 9(b). Therefore, the proposed method exploits the vectors adjacent to the output voltage reference vector in the space-vector plane. Compared to the approach used in the conventional SVPWM method, the output voltage reference can be synthesized more accurately, thus resulting in a reduction of output current ripples and harmonics. In contrast to the conventional SVPWM method, because a carrier-based PWM

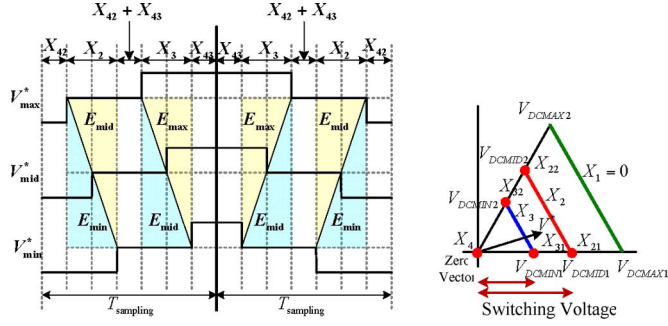


Fig. 10. New switching sequence with small output voltage reference using proposed method. (a) Switching sequence. (b) Effective voltage vector.

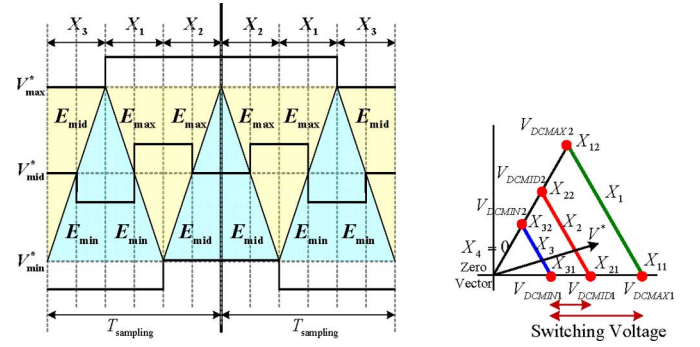


Fig. 11. New switching sequence with large output voltage reference using proposed method. (a) Switching sequence. (b) Effective voltage vector.

method concept similar to [7] is used, the proposed method can be implemented without the need for tables and/or complex calculations.

In the case of a small output voltage reference, the maximum input line-to-line voltage is not utilized. Hence, X_1 is then set to zero and X_2 , X_3 , and X_4 can be calculated from (13)–(16). A switching sequence to synthesize the output voltage is shown in Fig. 10. The effective duty ratio for each effective voltage vector X_{21} , X_{22} , X_{31} , and X_{32} can be calculated using (27)–(30) in the same manner as that described for the previous switching sequence. In addition, the distribution of the zero voltage vectors can be written as in (31) and (32)

$$X_2 = X_{21} + X_{22} \quad (27)$$

$$X_3 = X_{31} + X_{32} \quad (28)$$

$$X_{21} = X_2 \left(1 - \frac{V_{mid}^* - V_{min}^*}{V_{max}^* - V_{min}^*} \right) \quad (29)$$

$$X_{31} = X_3 \left(1 - \frac{V_{mid}^* - V_{min}^*}{V_{max}^* - V_{min}^*} \right) \quad (30)$$

$$X_{41} = \frac{1}{2} T_{\text{sampling}} X_4 \frac{V_{dcMID} X_2}{V_{dcMID} X_2 + V_{dcMIN} X_3} \quad (31)$$

$$X_{42} = \frac{1}{2} T_{\text{sampling}} X_4 \frac{V_{dcMIN} X_3}{V_{dcMID} X_2 + V_{dcMIN} X_3} \quad (32)$$

In the case of a large output voltage, X_4 is set to zero, which means that the zero vector is not used during the synthesis of the output voltage. A proper switching sequence for this situation is shown in Fig. 11. The effective duty ratios of every effective voltage vector X_{11} , X_{12} , X_{21} , X_{22} , X_{31} , and X_{32} can be calculated using (33)–(38). In this case, the number of commutations is five, while six commutations are used in the former two cases

$$X_1 = X_{11} + X_{12} \quad (33)$$

$$X_2 = X_{21} + X_{22} \quad (34)$$

$$X_3 = X_{31} + X_{32} \quad (35)$$

$$X_{11} = X_1 \left(1 - \frac{V_{mid}^* - V_{min}^*}{V_{max}^* - V_{min}^*} \right) \quad (36)$$

TABLE I

REGION OF SMALL OUTPUT VOLTAGE IN NEW SWITCHING SEQUENCE

$\alpha_o \backslash \beta_i$	0	$\frac{1}{6}\pi$
0	$0 \leq q \leq \frac{1}{\sqrt{3}}$	$0 \leq q \leq \frac{2}{3}$
$\frac{1}{6}\pi$	$0 \leq q \leq \frac{1}{2}$	$0 \leq q \leq \frac{1}{\sqrt{3}}$

$$X_{21} = X_2 \left(1 - \frac{V_{mid}^* - V_{min}^*}{V_{max}^* - V_{min}^*} \right) \quad (37)$$

$$X_{31} = X_3 \left(1 - \frac{V_{mid}^* - V_{min}^*}{V_{max}^* - V_{min}^*} \right) \quad (38)$$

C. Determination Between the Small and the Large Output Voltages

As described in the previous section, two kinds of new switching sequences are presented to reduce the output current harmonics. According to the magnitude of the output phase voltage, a new switching sequence with the small output voltage reference in Fig. 10, or the other switching sequence with the large output voltage reference in Fig. 11, can be selected.

The virtual dc-link voltages adjacent to the output voltage reference instantaneously vary according to the input-voltage phase angle, the output-voltage phase angle, and the voltage transfer ratio. Therefore, the criterion that determinate whether the output voltage is small or large, should also vary according to the aforementioned conditions. In the proposed method, the criterion is determined by a simple calculation. For example, when the output voltage reference is adjacent to the smallest virtual and the second largest virtual dc-link voltages, (13)–(16) can be satisfied under the condition of $X_1 = 0$, which means that the output voltage reference is small. On the other hand, if the effective duty ratios do not satisfy (13)–(16) with $X_1 = 0$, which means that the reference cannot be synthesized according to the switching sequence with small output voltage reference, and the output voltage reference is large. Therefore, the switching sequence with large output voltage reference is utilized. Table I shows the region of the proposed

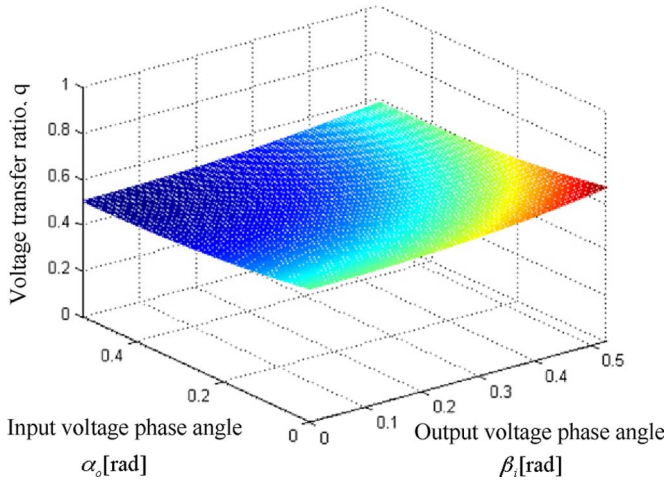


Fig. 12. Boundary of new switching sequence between the small and the large output voltage.

TABLE II
SIMULATION CONDITION

Quantity	Value [Unit]
R-L load	R=5 [Ω], L=0.2 [mH]
Input Voltage(line-to-line)	220 [Vrms]
Input Voltage Frequency	60 [Hz]
Input LC Filter	L=100 [μ H], C(Δ)=35 [μ F]
Output Voltage Frequency	30 [Hz]
Switching Frequency	10 [kHz]

switching sequence with the small output voltage reference, according to the input-voltage phase angle and output-voltage phase angle. The minimum boundary of the voltage transfer ratio of the small output voltage reference is 0.5 and the maximum boundary value is 0.667. The boundary surface between the small and large output voltage reference is illustrated in Fig. 12.

IV. SIMULATION RESULT

To evaluate the performance of the proposed method, simulations with an $R-L$ load were performed. The simulation conditions are shown in Table II.

Using the proposed method, a PWM switching sequence identical with that of the conventional PWM method was implemented. Additionally, to show the generality of the proposed PWM method, simulations using the new switching sequence to reduce the output current ripple were performed and the results are compared with those using the conventional PWM method.

A. Voltage Synthesis When Voltage Reference is Small

A small voltage reference means that the voltage transfer ratio (q) is small. As explained in Section III-B, the maximum virtual dc link was not utilized. Figs. 13 and 14 show the input

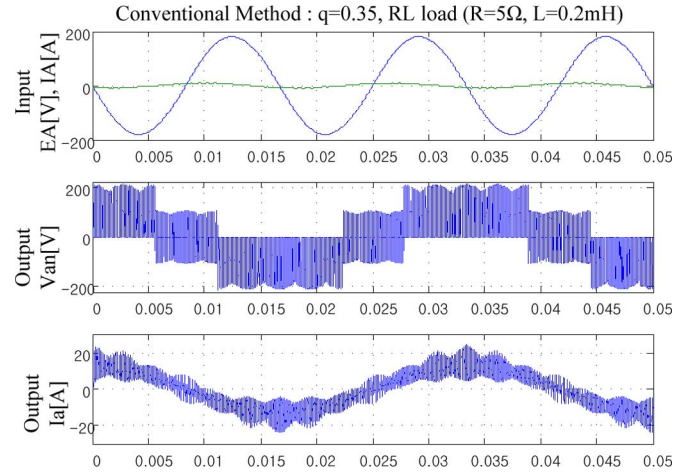


Fig. 13. Input voltage/current, output phase voltage, and output phase current with the conventional method at voltage transfer ratio = 0.35.

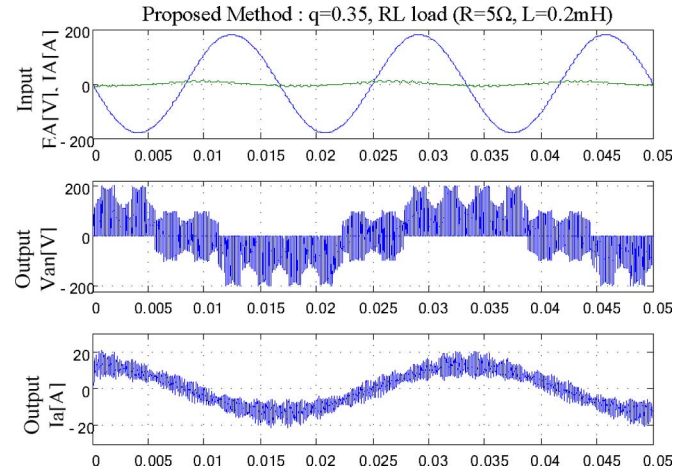


Fig. 14. Input voltage/current, output phase voltage, and output phase current with the proposed method at voltage transfer ratio = 0.35.

phase voltage and current, the output phase voltage, and the output phase current when the voltage transfer ratio was small ($q = 0.35$) using the conventional and proposed PWM methods, respectively.

The conventional PWM switching sequence used the maximum and medium virtual dc-link voltages, as well as the zero voltage to synthesize the voltage reference. However, the new switching sequence developed by the proposed method used the adjacent virtual dc-link voltages to reduce the output current ripple. The actual output voltages are shown in both figures. Using the new switching sequence, the voltage difference between the ON and OFF switching times was smaller than that produced by the conventional switching sequence, thus indicating that the output-current switching ripple can be reduced. Fig. 15 shows the harmonic characteristics of the output currents from the two PWM methods. The total harmonic distortion (THD) was improved and showed a reduction from 32.75% in the conventional method to 22.35% in the proposed method.

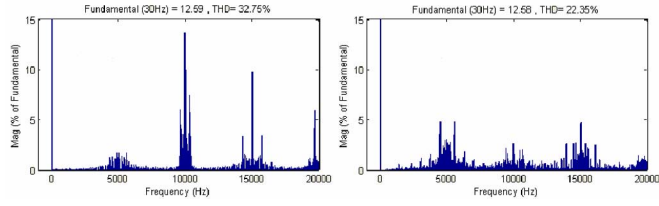


Fig. 15. Harmonic characteristics of output current at voltage transfer ratio = 0.35. (a) Conventional method. (b) Proposed method.

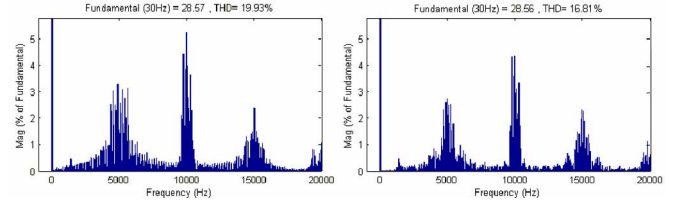


Fig. 18. Harmonic characteristics of output current at voltage transfer ratio = 0.8. (a) Conventional method. (b) Proposed method.

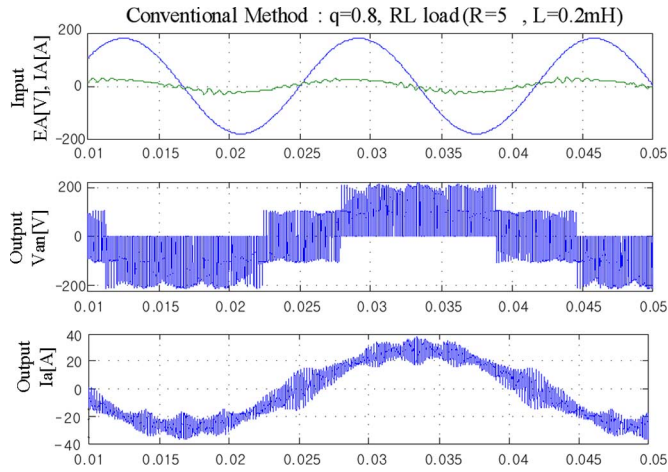


Fig. 16. Input voltage/current, output phase voltage, and output phase current with the conventional method at voltage transfer ratio = 0.8.

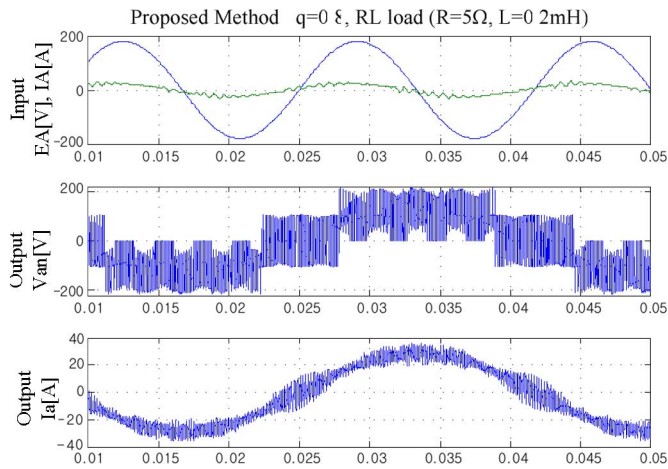


Fig. 17. Input voltage/current, output phase voltage, and output phase current with the proposed method at voltage transfer ratio = 0.8.

B. Voltage Synthesis When Voltage Reference is Large

Figs. 16 and 17 show the same waveforms as Figs. 13 and 14 under similar simulation conditions. However, in these simulations, the voltage transfer ratio was large ($q = 0.8$). The new switching sequence developed by the proposed method used the adjacent virtual dc link, thus resulting in a smaller amount of the output-current switching ripple. Fig. 18 shows the harmonic characteristics of the output current from the two PWM

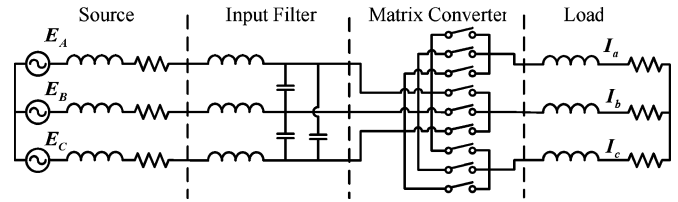


Fig. 19. Matrix converter configuration.

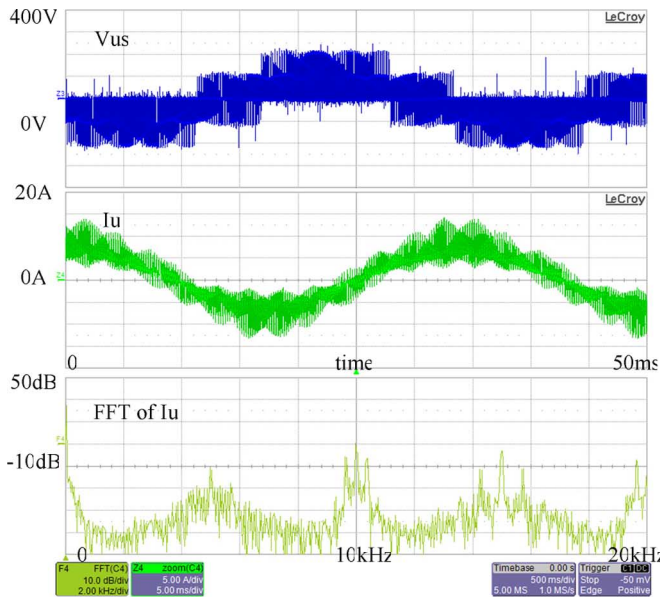
methods. The THD was improved with the results showing a reduction from 19.33% in the conventional method to 16.81% using the proposed method.

V. EXPERIMENTAL RESULT

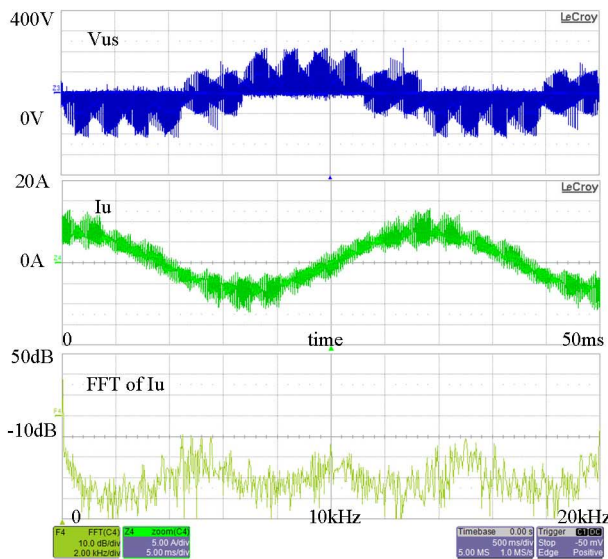
The diagram in Fig. 19 was implemented to verify the validity of the proposed PWM method. The loads were three-phase $R-L$ loads, whose parameters were 10Ω and 0.2 mH , and the ac source line-to-line rms voltage was 220 V . To compare the characteristics of the currents developed by the conventional and proposed switching sequences, the output currents were measured and their frequency spectra were also displayed.

Fig. 20 shows the output voltage and current waveforms when the output line-to-line rms voltage was 86 V and voltage transfer ratio was 0.39 , and its frequency was 30 Hz . Because the output voltage reference was small in Fig. 12, the proposed method used the smallest and the second largest virtual dc-link voltages, which meant that X_1 was set as 0 . Fig. 20(a) and (b) shows the results from the experiments with the conventional and proposed methods, respectively. The figures show, from the top, traces of the output phase voltage, the output current, and fast Fourier transform (FFT) results of the output current. Regardless of the magnitude of the output phase voltage reference, the conventional method uses the maximum and the medium virtual dc-link voltages. However, the proposed method selects the virtual dc-link voltage adjacent to the output phase voltage reference, so that X_1 is equal to 0 . Therefore, in the proposed method, the voltage difference between the ON and OFF switching period was smaller than that in the conventional method. As a result, output-current switching ripple was reduced. As expected, the proposed method in Fig. 20(b) produced smaller harmonics over the entire frequency range than the conventional method in Fig. 20(a).

Fig. 21 shows the voltage, current, and FFT results when the output line-to-line rms voltage was 147 V and voltage transfer



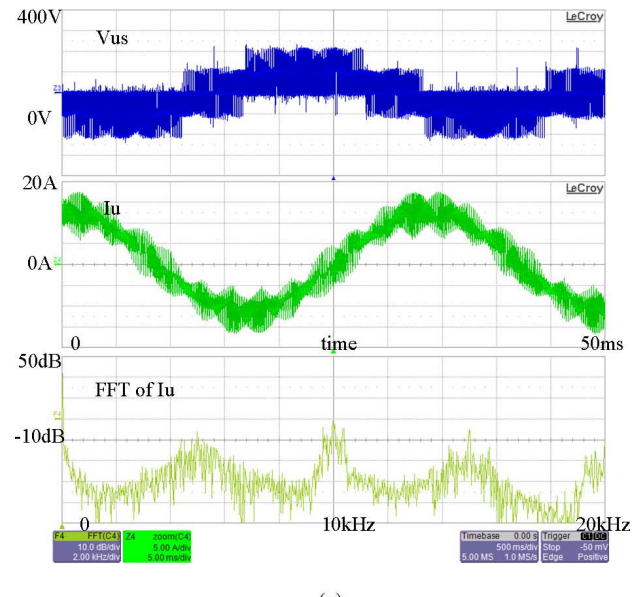
(a)



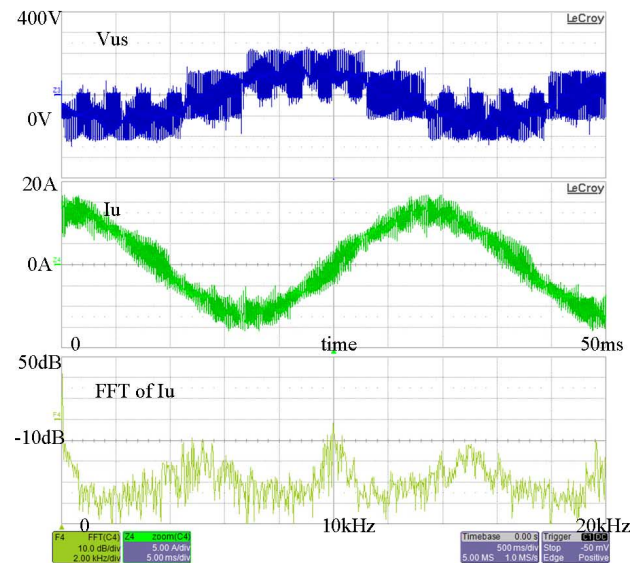
(b)

Fig. 20. Output switching voltage, output current, and FFT in small output voltage reference. (a) Conventional method. (b) Proposed method.

ratio was 0.67, and its frequency was 30 Hz. Because the output voltage reference was large in Fig. 12, the proposed method did not use the zero vector, which meant that X_4 was set as 0, which can be visually confirmed by comparing the output phase voltages in the first 10 ms of the traces in Fig. 21(a) and (b). These figures also show that the voltage difference between the ON and OFF switching times was smaller when using the proposed method than the conventional method. The output current waveforms and the associated FFT data indicate that the harmonics developed by the proposed PWM method was lower than those using the conventional PWM method, in spite of using less switching frequency. If the switching frequencies of



(a)



(b)

Fig. 21. Output switching voltage, output current, and FFT in large output voltage reference. (a) Conventional method. (b) Proposed method.

both methods are set as the same, the difference in the harmonic pattern would be conspicuous.

Fig. 22 shows the input current waveforms using the two methods when the output voltage conditions were small (output line-to-line rms voltage 86 V) and large (output line-to-line rms voltage 147 V). In a comparison with the input current waveforms of the conventional method, input current waveforms of the proposed method show more ripples. This is because to minimize the output current ripple, the proposed switching sequence does not consider the input-current harmonic characteristics. And, the input-current harmonic characteristics might be worse, even though this kind of virtual dc-link selection can improve the output-current harmonic characteristics conspicuously.

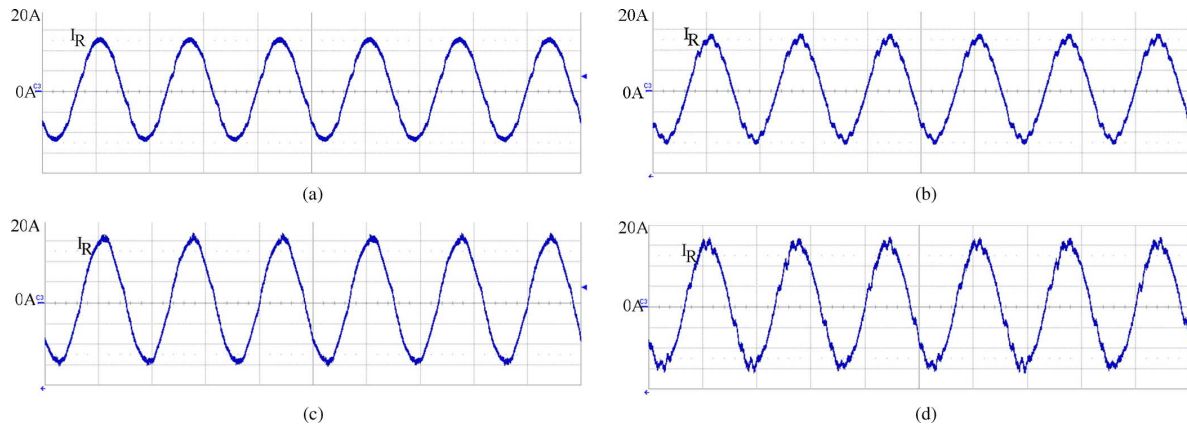


Fig. 22. Input current waveforms with the conventional method and the proposed method. (a) Conventional method in small output voltage. (b) Proposed method in small output voltage. (c) Conventional method in large output voltage. (d) Proposed method in large output voltage.

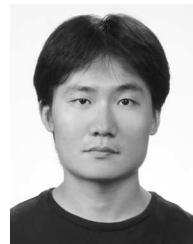
VI. CONCLUSION

This paper has presented a novel generalized PWM method for a matrix converter using the virtual dc-link concept. The proposed method takes advantages of the three hexagons of the virtual dc link of the matrix converter, while the conventional PWM has used only two of these hexagons. The proposed method can implement the same switching sequence as the conventional method. In addition, the new switching sequences that can reduce the output current ripple have been proposed as an application of the proposed method. As a result, the harmonic characteristics of the output current of the matrix converter were improved at the cost of some increase in input current ripples. The proposed method is compatible with the carrier-based PWM method, and it can be easily implemented without tables and complex calculations.

REFERENCES

- [1] A. Alesina and M. Venturini, "Solid-state power conversion: A fourier analysis approach to generalized transformer synthesis," *IEEE Trans. Circuits Syst.*, vol. CAS-28, no. 4, pp. 319–330, Apr. 1981.
- [2] D. Casadi, G. Grandi, G. Serra, and A. Tani, "Space vector control of matrix converters with unity input power factor and sinusoidal input/output waveforms," in *Proc. EPE Conf.*, 1993, vol. 7, pp. 170–175.
- [3] D. Casadi, G. Serra, A. Tani, and L. Zari, "Matrix converter modulation strategies: A new general approach based on space-vector representation of the switch state," *IEEE Trans. Ind. Electron.*, vol. 49, no. 2, pp. 370–381, Apr. 2002.
- [4] P. Ziogas, S. Khan, and M. Rashid, "Analysis and design of forced commutated cycloconverter structures with improved transfer characteristics," *IEEE Trans. Ind. Electron.*, vol. IE-33, no. 3, pp. 271–280, Aug. 1986.
- [5] L. Huber and D. Borjovic, "Space vector modulated three-phase to three-phase matrix converter with input power factor correction," *IEEE Trans. Ind. Appl.*, vol. 21, no. 6, pp. 1234–1246, Nov./Dec. 1995.
- [6] P. W. Wheeler, J. Rodriguez, J. C. Clare, L. Empringham, and A. Weinstein, "Matrix converter: A technology review," *IEEE Trans. Ind. Electron.*, vol. 49, no. 2, pp. 276–288, Apr. 2002.
- [7] Y. D. Yoon and S. K. Sul, "Carrier-based modulation technique for matrix converter," *IEEE Trans. Power Electron.*, vol. 21, no. 6, pp. 1691–1703, Nov. 2006.
- [8] P. Nielsen, F. Blaabjerg, and J. K. Pedersen, "Space vector modulated matrix converter with minimized number of switchings and a feedforward compensation of input voltage unbalance," in *Proc. PEDES*, 1996, vol. 2, pp. 833–839.
- [9] L. Helle, K. B. Larsen, A. H. Jorgensen, S. Munk-Nielsen, and F. Blaabjerg, "Evaluation of modulation schemes for three-phase to three-phase matrix converters," *IEEE Trans. Ind. Electron.*, vol. 51, no. 1, pp. 158–171, Feb. 2004.

- [10] J. W. Kolar and F. Schafmeister, "Novel modulation scheme minimizing the switching losses of sparse matrix converters," in *Proc. IECON Conf.*, 2003, vol. 3, pp. 2085–2090.
- [11] J. W. Kolar, F. Schafmeister, S. D. Round, and H. Ertl, "Novel three-phase AC–AC sparse matrix converters," *IEEE Trans. Power Electron.*, vol. 22, no. 5, pp. 1649–1661, Sep. 2007.
- [12] R. Vargas, J. Rodriguez, U. Ammann, and P. W. Wheeler, "Predictive current control of an induction machine fed by a matrix converter with reactive power control," *IEEE Trans. Ind. Electron.*, vol. 55, no. 12, pp. 4362–4371, Dec. 2008.
- [13] R. Vargas, U. Ammann, and J. Rodriguez, "Predictive approach to increase efficiency and reduce switching losses on matrix converters," *IEEE Trans. Power Electron.*, vol. 24, no. 4, pp. 894–902, Apr. 2009.
- [14] D. Casadei, G. Serra, A. Tani, and L. Zari, "Optimal use of zero vectors for minimizing the output current distortion in matrix converters," *IEEE Trans. Ind. Electron.*, vol. 56, no. 2, pp. 326–336, Feb. 2009.



Sungmin Kim (S'09) was born in Seoul, Korea, in 1980. He received the B.S. and M.S. degrees in electrical engineering from Seoul National University, Seoul, Korea, in 2002 and 2008, respectively, where he is currently working toward the Ph.D. degree.

His current research interests include power electronics control of electric machines, matrix converter drive, and power-conversion circuits.



Young-Doo Yoon (S'06) was born in Seoul, Korea, in 1978. He received the B.S. and M.S. degrees in electrical engineering from Seoul National University, Seoul, Korea, in 2002 and 2005, respectively, where he is currently working toward the Ph.D. degree.

His current research interests include power electronics control of electric machines, matrix converter drive, and ultraprecision motion control.



Seung-Ki Sul (S'78–M'80–SM'98–F'00) was born in Korea, in 1958. He received the B.S., M.S., and Ph.D. degrees in electrical engineering from Seoul National University, Seoul, Korea, in 1980, 1983, and 1986, respectively.

From 1986 to 1988, he was an Associate Researcher in the Department of Electrical and Computer Engineering, University of Wisconsin, Madison. From 1988 to 1990, he was a Principal Research Engineer in Gold-Star Industrial Systems Company. Since 1991, he has been a member of the Faculty of the School of Electrical Engineering, Seoul National University, where he is currently a Professor. His research interests include power-electronic control of electric machines, electric/hybrid vehicle drives, and power-converter circuits.